Electrochemical and Solid-State Letters, **6** (1) C4-C7 (2003)
0013-4651/2002/6(1)/C4/4/$7.00 © The Electrochemical Society, Inc.

Electrochemical Etching of Individual Multiwall Carbon Nanotubes

Takashi Ito, Li Sun, and Richard M. Crooks*,z

Department of Chemistry, Texas A&M University, College Station, Texas 77842, USA

The electrochemical properties of individual multiwall carbon nanotubes (MWNTs) coated with an amorphous carbon layer are reported. MWNTs were etched at potentials more positive than 1.7 V *vs.* Ag/AgCl (3 M NaCl) in an aqueous 0.1 M KCl electrolyte solution. The logarithm of etching rate was proportional to the applied electrode potential, suggesting a kinetic etching mechanism. The estimated charge necessary to etch a MWNT was smaller than the total charge passed during etching, indicating that current was consumed for other parasitic reactions. Transmission electron microscopy (TEM) images of partially etched MWNTs indicate that etching begins at the distal end and proceeds preferentially along the longitudinal axis of the nanotube. The amorphous carbon layer was etched more readily than the graphitic core. TEM images of completely etched MWNTs showed that the pore at the distal end was still open, and that the tip of the MWNT was sharpened. These results indicate that electrochemical etching might be useful for controlling the shape and length of carbon nanotubes.

[DOI: 10.1149/1.1526779]

Manuscript submitted July 11, 2002; revised manuscript received October 1, 2002. Available electronically November 13, 2002.

Here, we report on the electrochemical properties of individual multiwall carbon nanotubes (MWNTs) in an aqueous electrolyte solution. The nanotubes used in this study have a pore diam of about 100 nm and are coated with amorphous carbon. We chose to examine these materials because individual nanotubes of this size and composition can be manipulated relatively easily. Understanding the electrochemical properties of individual carbon nanotubes (CNTs), particularly their etching properties, is important for a number of reasons. First, electrochemical data derived from individual NTs can be correlated directly and quantitatively to information obtained from other analytical methods, such as microscopy. Second, it may be possible to use electrochemical methods to control the size and shape of individual CNTs, which will likely be necessary if they are to be incorporated into devices of various sorts.[1] Third, many proposed applications of CNTs require an understanding of their stability and corrosion properties.

We have shown that individual MWNTs could serve as electrodes.[2] More recently, we have become interested in the use of CNTs for preparing single-pore membranes.[3] Such membranes have been used to construct Coulter counters,[4] which also enable study of transport phenomena within CNTs. Electrical approaches to particle counting, such as that employed by Coulter-type devices, require application of an electrical potential across a single-pore membrane. The potential drives a current that is carried by ions migrating through the pore. However, when a sufficiently large potential is applied across a conductive pore, such as a CNT, it is possible for a faradaic electrochemical process to carry all or part of the current, because the CNT acts as a bipolar electrode.[5,6] Because only ionic current carries analytical information in a Coulter counter, optimization of the CNT-based membranes necessitates an understanding of the potential range over which Faradaic processes are minimized. Knowledge of the electrochemical properties of CNTs is important for other potential applications too; these include catalysis of redox reactions,[7-11] electrochemical hydrogen storage,[12] Li intercalation,[13,14] and electrochemical capacitors.[15,16]

In this report we describe the electrochemical properties of individual MWNTs coated with an amorphous carbon layer. We found that MWNTs etched in 0.1 M KCl at potentials more positive than 1.7 V *vs.* Ag/AgCl (3M NaCl). The extent of etching could be easily controlled by adjusting the immersion depth of the MWNT in the electrolyte solution and the applied electrode potential. The electrochemical and electron microscopy data described in this paper are interpreted in terms of a model that accounts for the observed etching behavior. Electrochemical etching of CNTs represents a new method for controlling the length and width of CNTs that complements existing methods such as gas-[17] and solution-phase chemical etching,[18,19] and cutting with electrical discharges.[20,21]

Experimental

Chemicals and materials.—All solutions were prepared with water having a resistance of 18.2 MΩ cm (Milli-Q, Millipore). KCl, H_2SO_4, and H_2O_2 (EM Sciences, Gibbstown, NJ) were of reagent grade quality or better and used without further purification. MWNTs, produced via a chemical vapor deposition process,[22] were used as received from Applied Sciences (Cedarville, OH).

Fabrication of MWNT electrodes.—With the aid of an optical microscope (100-600 times magnification, Optiphot, Nikon, Tokyo), a single MWNT was removed from its bundle using a sharp Pt tip having acrylic adhesive (adhesive carbon tape, Ted Pella Inc., Redding, CA) on its apex. The junction between the MWNT and the metal tip was then coated with Ag epoxy (Epoxy Technology Inc., Billerica, MA) to improve electrical contact.[2] An xyz translational stage (model 462: Newport, Irvine, CA) was used to perform these manipulations. Prior to electrochemical experiments, the surfaces of MWNT electrodes were cleaned by dipping in a freshly prepared piranha solution for several seconds (3:1 concentrated H_2SO_4:30% H_2O_2).

Safety note: Piranha solution reacts violently with organic compounds and should not be stored in closed containers.

Electrochemistry and microscopy.—Electrochemical data were obtained using either a Pine Instruments model AFRDES bipotentiostat (Grove City, PA), a Bioanalytical Systems model 100B electrochemical analyzer (West Lafayette, IN), or a CH Instruments model 660A electrochemical analyzer (Austin, TX). Electrochemical experiments were carried out in a three-electrode cell (Fig. 1) containing an Ag/AgCl (3 M NaCl) reference electrode, and a Pt counter electrode. One end of a single 60-270 μm long MWNT electrode was dipped into a drop of an aqueous electrolyte solution (typical immersion depth: 10-70 μm) defined by a small hole (~0.8 mm diam) in a Teflon block (Fig. 1). With this design it was not possible to exclude oxygen from the electrolyte solution.

Optical micrographs of MWNTs were recorded using an inverted microscope (TE 300, Nikon) equipped with a 2D charge-coupled device array detector (SenSys 1401E, Photometrics, Tucson, AZ). Transmission electron microscope (TEM) and energy dispersive X-ray spectroscopy (EDS) measurements of MWNTs fixed at the apex of metal tips were obtained using a JEM-2010 microscope (JEOL, Tokyo, Japan).

---

* Electrochemical Society Active Member.

[z] E-mail: crooks@tamu.edu

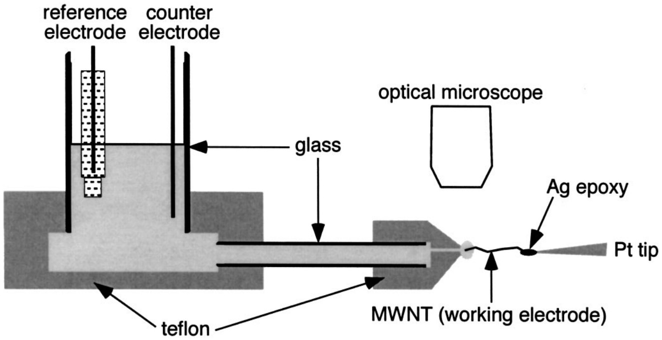

Figure 1. Schematic illustration of the experimental apparatus used to etch individual MWNTs.

Results and Discussion

Figure 2 shows a typical cyclic voltammogram obtained using a single MWNT electrode in an aqueous 0.1 M KCl electrolyte solution. The data indicate no voltammetric peaks in the range -0.5 to 1.3 V, but beyond this range significant cathodic and anodic currents are observed. The onset of cathodic current is about 0.5 V more positive than previously reported values (about -1.0 V) for macroscopic carbon electrodes[23,24] or for single-wall CNT sheet electrodes in aqueous electrolyte solutions.[13,14,25] Bubbles are observed on the MWNT electrode at potentials more negative than -0.5 V, and therefore H_2 evolution is the likely faradaic process responsible for the negative potential limit. The relatively positive voltage onset for H_2 generation may be a consequence of the presence of metallic impurities such as Fe, which is used as a catalyst during the synthesis of the MWNTs.[22] However, if such impurities are present, they are below the detection limit of EDS. In addition to proton reduction, the current observed at negative potentials may partially arise from reduction of oxygen, which is not excluded from the electrolyte.[26]

The onset potential for anodic current is 1.3 V, and at potentials higher than 1.7 V, MWNTs and the surrounding amorphous carbon layer begin to etch. In contrast, anodic oxidation of highly ordered pyrolytic graphite and glassy carbon electrodes leads to formation of a surface oxide and surface roughening under similar conditions.[24]

Figures 3a and b are optical micrographs of a MWNT before and after electrochemical etching, respectively, for 24 min at 1.8 V in aqueous 0.1 M KCl. The immersed part of the MWNT (the electrolyte solution level is indicated by an arrow in Fig. 3a) was completely removed under these conditions. Because this result is highly reproducible, we conclude that this electrochemical method provides a means for controlling the length of MWNTs. Figure 3c shows a TEM image of the distal end of an etched MWNT. The important information here is that the end of the MWNT is open and the wall thickness is reduced at the end of the tube that was exposed to the etching solution.

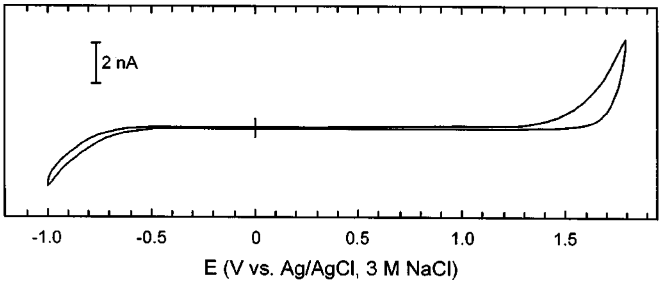

Figure 2. A typical CV for an individual MWNT electrode (outer diam: 240 nm, pore diam: 80 nm, immersion depth: 30 μm) in aqueous 0.1 M KCl. Scan rate: 100 mV/s.

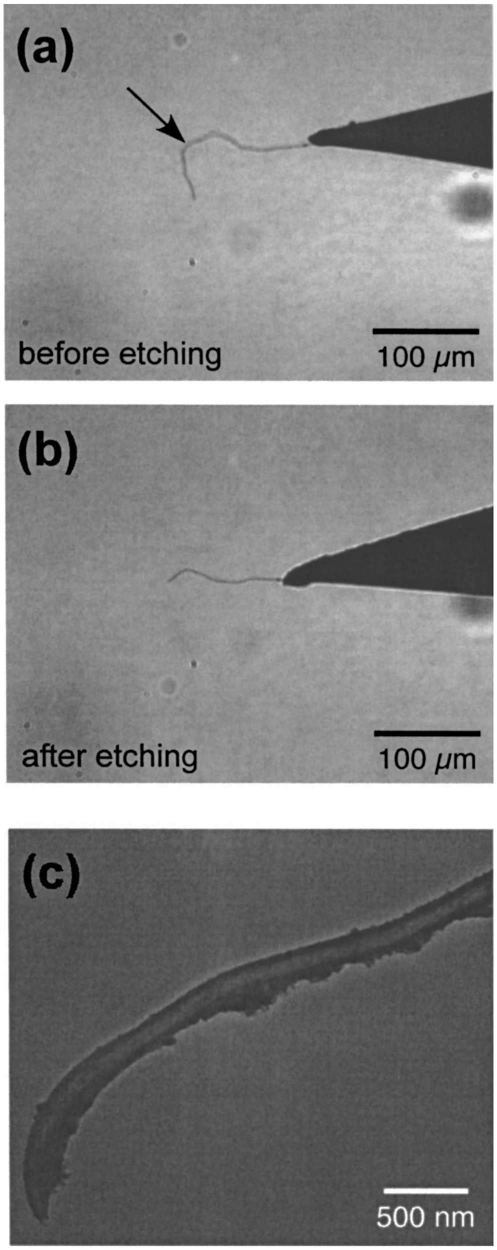

Figure 3. Optical micrographs of a single MWNT electrode (a) before and (b) after electrochemical etching. (c) TEM of the distal end of a completely etched MWNT.

To learn more about the etching process, a MWNT electrode was characterized by chronoamperometry. Figure 4a shows typical chronoamperograms after the electrode potential was stepped from 0 to 2 V (black line) and from 0 to 1.9 V (gray line). The results of measurements such as these were reproducible when different fractions of the same MWNT were etched, but the absolute etching time varied as a function of the particular MWNT used for the experiment. This is probably a consequence of slight variations in wall thickness. Nevertheless, the shapes of these chronoamperograms were similar to each other.

Two distinct regions are observed in the chronoamperograms. The current in the first region decreases at a faster rate (see inset) than it does in the second region. We speculate that the initial large current ($t < 5$ s) may be due to a combination of processes such as

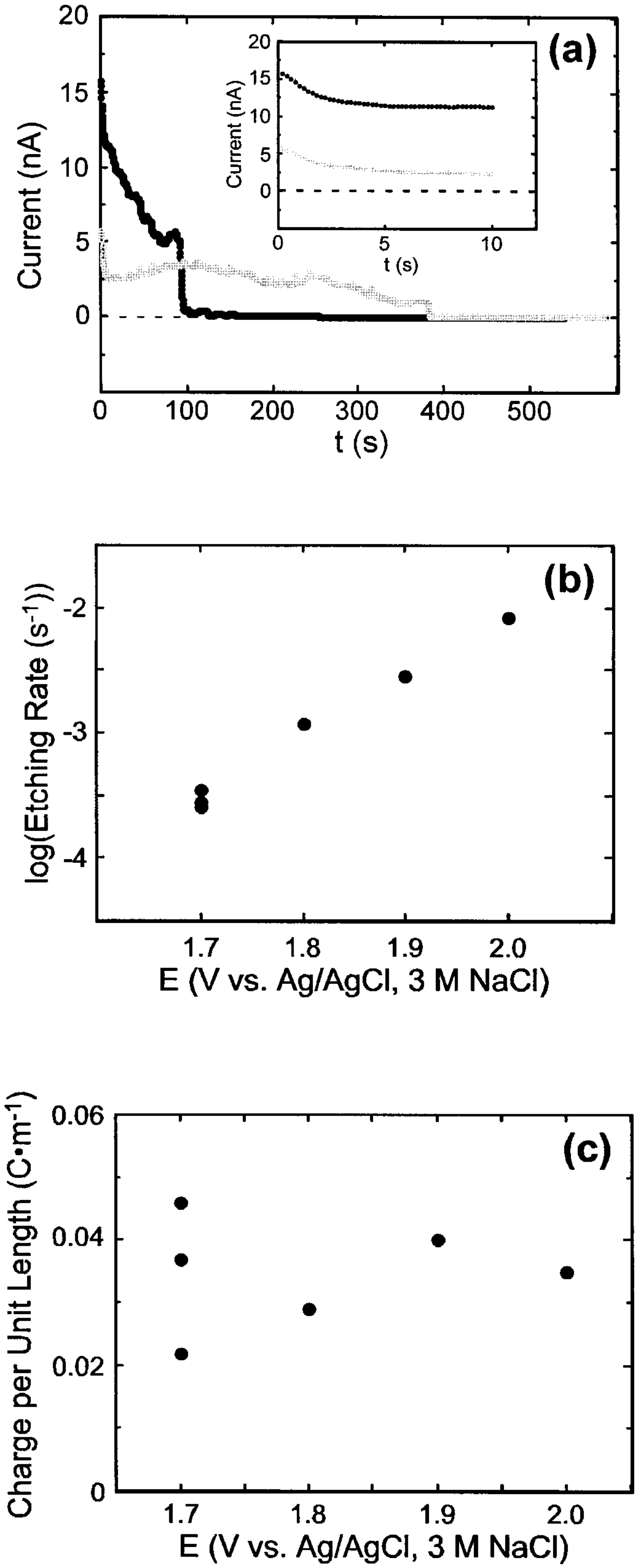

Figure 4. (a) Typical chronoamperometric response from a single MWNT electrode (outer diam: 220 nm, pore diam: 70 nm, immersion depth: 20 μm) for potential steps from 0 to 2 V (black line) and from 0 to 1.9 V (gray line). (b) Relationship between the logarithm of etching rate for a constant immersion depth (20 μm) and the applied electrode potential, *E*. (c) Relationship between total charge consumed during etching and *E*. All data shown in this figure were obtained with different fractions of the same MWNT in an aqueous 0.1 M KCl electrolyte solution.

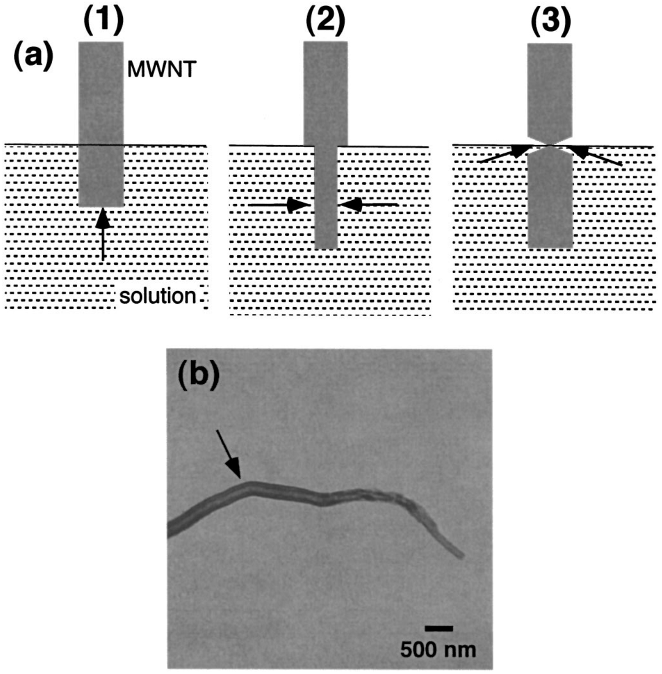

Figure 5. (a) Possible electrochemical etching mechanisms for MWNTs: (1) longitudinal etching from the distal to the proximal end; (2) uniform etching perpendicular to the longitudinal axis of the nanotube; (3) preferential etching at the air/electrolyte solution interface. (b) TEM image of the distal end of a partially etched MWNT. The electrolyte solution level is indicated by the arrow.

slow capacitive charging, surface faradaic reactions, and superficial intercalation.[24] The gradual decrease in the oxidation current reflects a decrease in the surface area of the MWNT as it etches. Irregular changes in the oxidation current as a function of time are probably due to vibration of the nanotube, which leads to slight changes in the immersion depth and fluctuations in the electrical noise.

In Fig. 4a, the etching time, defined as time required for the current to reach zero, was shorter at 2 V (120 s) than at 1.9 V (350 s). Indeed, the etching rate (1/etching time) for a constant immersion depth (20 μm) was higher at higher applied potentials over the range 1.7 to 2 V (Fig. 4b). At potentials less than 1.7 V, etching did not occur or was too slow to be reliably measured. The logarithm of the etching rate was almost linearly dependent on the applied potential, which implies a kinetically controlled etching mechanism.[23] The charge required to etch a unit length of an MWNT electrode, determined by integrating the chronoamperometric response and normalizing to the etched length, is, at the indicated level of reproducibility, independent of the applied potential in the range between 1.7 and 2 V (Fig. 4c). This charge (~0.04 C/m) is about 18 times larger than the calculated charge required for complete oxidation of the MWNT (2.2×10^{-3} C/m, assuming that all carbon is converted to carbon dioxide). This indicates that current is consumed for both oxidative etching of the MWNT and simultaneously for other anodic reactions such as oxidation of water.

There are three possible electrochemical etching mechanisms for MWNTs (Fig. 5a). First, the nanotube could be etched linearly from the distal to the proximal end. Second, the MWNT could be etched uniformly from the periphery toward the inner graphitic core. Third, the nanotube could be etched selectively at the air/electrolyte solution interface; in this case, the distal end of the nanotube would simply fall into the solution when etching is complete.

TEM images for four different MWNTs at various stages during the etching process were obtained to differentiate between these three possibilities. A TEM of one of these four MWNTs is shown in Fig. 5b. Very similar TEM images were obtained for two of the other MWNTs, but the etching behavior of the fourth MWNT was somewhat different (*vide infra*). The image in Fig. 5b was obtained from a nanotube immersed in the electrolyte solution to a depth of ~15 μm. Etching was terminated after passing a charge of 0.39 μC, which we estimate to be about 65% of that required for complete etching. After etching, 10 μm of the MWNT length was removed and 5 μm remained (the electrolyte solution level is indicated by an arrow in Fig. 5b). Importantly, the distal end of the MWNT was thinned, whereas the portion near the solution level remained intact. These observations indicate that etching starts at the distal end of the MWNT and proceeds simultaneously via the mechanisms shown in frames 1 and 2 of Fig. 5a. Moreover, examination of the distal end of the MWNT indicates that the amorphous carbon layer etches more quickly than the graphitic core.

In contrast to the behavior discussed in the foregoing paragraph, which is representative of three of the four partially etched MWNTs, the remaining MWNT etched selectively at the air/electrolyte solution interface (data not shown). We suspect that this nanotube contained a defect site at the air/electrolyte solution interface, but the point is that under some conditions the etching mechanism represented by frame 3 may be operative.

Consistent with our general model for etching, which is a combination of the mechanisms shown in frames 1 and 2 of Fig. 5a, we also observed that an increase in immersion depth resulted in a longer etching time. However, this time varied from nanotube to nanotube and was not necessarily directly proportional to the immersion depth. Taken together with the TEM results shown in Fig. 5, we conclude that electrochemical etching usually starts at the distal end of the MWNT, probably because the electric field is highest there. This results in selective etching along the longitudinal axis of the MWNT, but etching also occurs at a measurable rate perpendicular to the longitudinal axis. We hypothesize that etching occurs as a consequence of carbon oxidation via an intermediate generated at the MWNT surface when H_2O is converted to oxygen.[27]

Conclusions

In this study, we described the electrochemistry of individual MWNTs in aqueous electrolyte solutions. The most interesting results were obtained at positive potentials where the MWNTs were etched. Etching started from the amorphous carbon layer at the distal end of the MWNT and proceeded longitudinally toward the proximal end. Slower etching was also observed perpendicular to this direction. The etching rate and length are determined by the electrode potential and the immersion depth, respectively. This provides a means for controlling the geometry of nanotubes. For example, this etching method may be useful for removing CNT templates used to prepare nanopores without damaging the surrounding polymeric membrane matrix.[28] It might also be possible to selectively remove the amorphous carbon layer of a MWNT from the graphitic core. Details of the reactions responsible for etching of the MWNTs are not clear at present, but they may be clarified by investigating the effects of a variety of factors such as dissolved O_2 concentration, solution pH, and electrolyte composition.

Acknowledgments

We gratefully acknowledge financial support from the U.S. Department of Energy (contract no. DE-FG03-01ER15247). We thank Dr. Zhiping Luo (Microscopy and Imaging Center, Texas A&M University) for his assistance with TEM imaging and EDS measurements. We also thank Dr. D. G. Glasgow (Applied Sciences, Inc., Cedarville, OH) for providing the CNTs used in this study.

Texas A&M University assisted in meeting the publication costs of this article.

References

1. P. J. F. Harris, *Carbon Nanotubes and Related Structures*, Cambridge University Press, Cambridge, U.K. (1999).
2. J. K. Campbell, L. Sun, and R. M. Crooks, *J. Am. Chem. Soc.*, **121**, 3779 (1999).
3. L. Sun and R. M. Crooks, *J. Am. Chem. Soc.*, **122**, 12340 (2000).
4. R. W. Lines, in *Particle Size Analysis*, N. G. Stanley-Wood and R. W. Lines, Editors, p. 351, Royal Society of Chemistry, Cambridge, U.K. (1992).
5. M. Fleischmann, J. Ghoroghchian, D. Rolison, and S. Pons, *J. Phys. Chem.*, **90**, 6392 (1986).
6. A. Arora, J. C. T. Eijkel, M. E. Morf, and A. Manz, *Anal. Chem.*, **73**, 3282 (2001).
7. P. J. Britto, K. S. V. Santhanam, and P. M. Ajayan, *Bioelectrochem. Bioenerg.*, **41**, 121 (1996).
8. J. J. Davis, R. J. Coles, and H. A. O. Hill, *J. Electroanal. Chem.*, **440**, 279 (1997).
9. P. J. Britto, K. S. V. Santhanam, A. Rubio, J. A. Alonso, and P. M. Ajayan, *Adv. Mater.*, **11**, 154 (1999).
10. J. M. Nugent, K. S. V. Santhanam, A. Rubio, and P. M. Ajayan, *Nano Lett.*, **1**, 87 (2001).
11. H. Luo, Z. Shi, N. Li, Z. Gu, and Q. Zhuang, *Anal. Chem.*, **73**, 915 (2001).
12. X. Qin, X. P. Gao, H. Liu, H. T. Yuan, D. Y. Yan, W. L. Gong, and D. Y. Song, *Electrochem. Solid-State Lett.*, **3**, 532 (2000).
13. J. N. Barisci, G. G. Wallace, and R. H. Baughman, *Electrochim. Acta*, **46**, 509 (2000).
14. J. N. Barisci, G. G. Wallace, and R. H. Baughman, *J. Electroanal. Chem.*, **488**, 92 (2000).
15. C. Niu, E. K. Sichel, R. Hoch, D. Moy, and H. Tennent, *Appl. Phys. Lett.*, **70**, 1480 (1997).
16. C.-Y. Liu, A. J. Bard, F. Wudl, I. Weitz, and J. R. Heath, *Electrochem. Solid-State Lett.*, **2**, 577 (1999).
17. D. B. Hawhinney, V. Naumenko, A. Kuznetsova, J. T. Yales, Jr., J. Liu, and R. E. Smalley, *J. Am. Chem. Soc.*, **122**, 2383 (2000).
18. J. Liu, A. G. Rinzler, H. Dai, J. H. Hafner, R. K. Bradley, P. J. Boul, A. Lu, T. Iverson, K. Shelimov, C. B. Huffman, F. Rodriguez-Macias, Y.-S. Shon, T. R. Lee, D. T. Colbert, and R. E. Smalley, *Science*, **280**, 1253 (1998).
19. K. Hernadi, A. Siska, L. Thiên-Nga, L. Forró, and I. Kiricsi, *Solid State Ionics*, **141-142**, 203 (2001).
20. H. Dai, J. H. Hafner, A. G. Rinzler, D. T. Colbert, and R. E. Smalley, *Nature (London)*, **384**, 147 (1996).
21. J. Cumings, P. G. Collins, and A. Zettl, *Nature (London)*, **406**, 586 (2000).
22. G. G. Tibbetts, G. L. Doll, D. W. Gorkiewicz, J. J. Moleski, T. A. Perry, C. J. Dasch, and M. J. Balogh, *Carbon*, **31**, 1039 (1993).
23. A. J. Bard and L. R. Faulkner, *Electrochemical Methods, Fundamentals and Applications*, Wiley, New York (1980).
24. R. L. McCreery, in *Electroanalytical Chemistry*, A. J. Bard, Editor, Vol. 17, p. 221, Marcel Dekker, New York (1991).
25. J. N. Barisci, G. G. Wallace, and R. H. Baughman, *J. Electrochem. Soc.*, **147**, 4580 (2000).
26. H.-H. Yang and R. L. McCreery, *J. Electrochem. Soc.*, **147**, 3420 (2000).
27. J. O. Besenhard, J. Jakob, U. Krebber, P. Moeller, R. F. Sauter, A. Kurtze, N. Kanani, H. Meyer, J. K. H. Hoerber, and A. D. Jannakoudakis, *Z. Naturforsch. B*, **44**, 729 (1989).
28. L. Sun and R. M. Crooks, *Langmuir*, **15**, 738 (1999).